Flow Induced at a Wall by a Vortex Pair

S. Ersoy* and J. D. A. Walker†
Lehigh University, Bethlehem, Pennsylvania

The motion of a counter-rotating pair of two-dimensional vortices above a plane wall is considered. The vortices are assumed to be initially placed in an otherwise stagnant and incompressible fluid above the wall. Depending on the assumed sense of rotation, the vortices either recede from the wall or move toward it, at an angle of attack; both situations are considered. Numerical solutions are obtained for the unsteady viscous boundary-layer flow that develops on the wall due to the vortex motion. In all cases, separation occurs in the boundary layer in the form of the appearance of secondary eddies; in addition, explosive boundary-layer growth is invariably observed near these eddies. The results suggest that the boundary-layer flow will ultimately erupt into the inviscid region in a strong viscous-inviscid interaction with the outer flow. The relation of these results to recent experimental work is discussed.

Nomenclature

a	= asymptotic separation distance of vortices, Eq. (1)
b	= initial separation distance of vortices
G	= coefficient defined by Eq. (26)
ℓ	= initial distance of vortices from wall, see Fig. 1
P, Q, R	= coefficients defined by Eqs. (22-25)
Re	= Reynolds number
t	= time
u	= tangential boundary-layer velocity
U_∞	= mainstream velocity defined by Eq. (11)
U	= velocity defined by Eq. (21)
U_1, U_2	= velocities defined by Eq. (12)
v	= normal boundary-layer velocity
V_{disp}	= displacement velocity defined by Eq. (36)
x_+	= quantity defined by Eq. (8)
x, y	= Cartesian coordinates
$(x_1, y_1), (x_2, y_2)$	= position of vortices 1 and 2, respectively, see Fig. 1
y_+	= quantity defined by Eq. (7)
α	= angle of attack of vortex pair, see Fig. 1
β	= angle of approach of vortex pair, see Fig. 2
ϵ	= vertical separation distance of vortices, Eq. (3)
κ	= vortex circulation
λ	= ratio defined by Eq. (5)
ξ	= streamwise coordinate defined by Eq. (17)
η	= coordinate defined by Eq. (18)
Ψ	= function defined by Eq. (19)
ψ	= two-dimensional stream function

I. Introduction

COUNTER-ROTATING vortex pairs occur in a wide variety of physical applications; for example, such vortices are observed trailing from the wings of aircraft in flight and in the outer region of laminar boundary layers on curved surfaces (Görtler vortices). In recent years, it has become evident that vortex motions play an important role in the dynamics of the time-dependent flow in a turbulent boundary layer. Consequently there has been considerable interest in attempting to define which types of vortex motions play the dominant role in the physics of the turbulent boundary layer and further to understand the types of flows these moving vortices induce. A variety of conceptual models have been proposed as dominant features of the flow in the near-wall region of the turbulent boundary layer; these include: 1) stretched hairpin vortices,[1-3] 2) long counter-rotating vortex pairs aligned in the streamwise direction,[4-7] and 3) discrete convected-loop vortices.[8-10] At present, it has not been possible to delineate definitively a predominant type of vortex structure from the experimental work and thereby to formulate a self-consistent description of the cyclic processes observed in the wall layer of a turbulent boundary layer. However, the recognition that vortices play an important role in the processes involved has led to some rather fundamental studies of vortex-induced boundary-layer flows. In particular, experimental studies of the effects of line vortices[12,13] and theoretical investigations of the boundary-layer flow induced by convected two-dimensional vortices[14,15] show that when a vortex is convected close to a solid wall, it is ultimately able to actuate a strong eruption of the boundary-layer flow. The moving line vortex generally induces a region of adverse pressure gradient near the wall, and here an unsteady separation effect occurs within the boundary layer; the separation is often in the form of secondary eddies. In the present paper, the term separation denotes the first appearance of a closed recirculating eddy within the boundary-layer flow (corresponding to the classical definition of boundary-layer separation[14]); it should be noted that the term "separation" is sometimes used by other authors[16] to denote the phenomenon of boundary-layer "breakaway," in which the boundary layer interacts strongly with the outer inviscid flow. Soon after separation, explosive boundary-layer growth occurs locally,[12,14,15] leading to a strong viscous-inviscid interaction between the boundary layer and the outer inviscid flow; the interaction involves an ejection of fluid from the boundary layer and often includes the production of secondary vortices.[12] This phenomenon is very similar to the bursting process observed in the near-wall region of the turbulent boundary layer.[8,15] It suggests providing an explanation of the basic physical mechanism for turbulence production near a solid wall; in this regenerative process, new vorticity is continually introduced into the outer layer of a turbulent boundary layer through intermittent ejections of fluid from the wall layer.

The observation of apparently compact ringlike vortex structures in the near-wall region of a turbulent boundary layer has led Falco,[9,11] Falco and Wiggert,[10] and Cerra and

Received May 7, 1985; presented as Paper 85-1583 at the AIAA 18th Fluid Dynamics, Plasmadynamics and Lasers Conference, Cincinnati, OH, July 14-18, 1985; revision received Feb. 3, 1986.

*Research Assistant, Department of Mechanical Engineering and Mechanics; currently Assistant Professor, Izmir University, Turkey.
†Professor, Department of Mechanical Engineering and Mechanics. Member AIAA.

Smith[17] to carry out some fundamental experiments in which the movement of a vortex ring toward a wall was observed. Once the vortex approached the wall, a strong unsteady separation was invariably observed in the boundary-layer flow near the wall. The process culminated in the ejection of a vortex structure from the wall region; the nature of the secondary vortex depends on the original orientation of the vortex and whether the fluid above the wall is originally stagnant or in motion (with an established boundary layer on the wall).

In most of the experiments of Falco and Wiggert,[10] Falco,[11] and Cerra and Smith,[17] the vortex generator was inclined at an angle to the wall; as a vortex ring is created by rapidly depressing the piston in the vortex generator, it quickly distorts into a rubber-band loop shape as it moves toward the wall. The calculation of the boundary-layer flow induced by such a moving vortex loop is made difficult owing to the fact that the flow is three-dimensional and unsteady; moreover, a relatively large computer would be required so that a sufficient number of mesh points could be used to ensure reasonable accuracy in a rapidly evolving and relatively complex boundary-layer flow. Fortunately a two-dimensional simulation of such flows can be carried out, and this is part of the motivation of this study.

The vortices in the studies by Falco and Wiggert,[10] Falco,[11] and Cerra and Smith[17] have a plane of symmetry that splits the vortex in half (and whose normal points in the spanwise direction). It is often convenient to carry out flow visualization in this plane of symmetry[17] and here, with the vortex cut in two places, the vortex motion appears to be due to two downward-moving counter-rotating vortices. Consequently, a reasonable simulation of the events in the symmetry plane may be achieved by considering the motion of a rectilinear vortex pair toward the wall and computing the boundary-layer development near the wall. This problem is addressed herein.

A vortex loop with the opposite sense of circulation from those considered by Falco and Wiggert,[10] Falco[11] and Cerra and Smith[17] will recede from the wall; such vortex configurations are difficult to generate artificially above a wall but may occur naturally in a turbulent wall-layer flow. Consequently, the boundary layer due to a counter-rotating pair of vortices that recede from the wall will also be considered here.

In the present paper, the motion of a pair of counter-rotating vortices that either approach the wall or recede from it at angle of attack is computed for an otherwise stagnant fluid. The development of the unsteady boundary-layer flow near the wall is calculated numerically. A variety of unusual and complex separation phenomena are revealed in the calculated results; in all cases, secondary vortices are produced in the boundary-layer flow. The results strongly suggest that an eruption of the boundary-layer flow will occur in the form of the ejection of the secondary vortices into the outer inviscid region.

II. The Inviscid Flow

Consider the initial configuration consisting of two counter-rotating rectilinear vortices above a plane wall as indicated in Fig. 1. In this study, rectilinear vortices were used rather than vortex models with finite cores. The flow induced by either type of vortex will be comparable at locations remote from the core and, since the main interest in this study was in the flow induced by the vortices near the wall, rectilinear vortices were used for mathematical convenience. The vortices are initially separated by a distance $2b$; the normal bisector of the line joining the two vortices intersects the wall at an angle α, which is subsequently referred to as the angle of attack. The parameter ℓ measures distance along the bisector to the plane wall; in addition (x^*, y^*) measure distance in directions tangential and normal to the wall, respectively. In the basic configuration assumed in Fig. 1, the vortex at (x_1^*, y_1^*) is always farthest from the wall, has rotation $+\kappa$, and is subsequently referred to as the first vortex. The second vortex at (x_2^*, y_2^*) is always closest to the wall and has rotation $-\kappa$; the image vortices have the rotations and locations indicated in Fig. 1. The vortex pair depicted in Fig. 1 will move toward the wall whereas, if the sense of all rotations is reversed, the pair will recede from the wall.

The equations governing the subsequent trajectories of the vortices can be readily obtained[18] using the fact that each vortex is convected in the velocity field of the other vortex and the two image vortices. These equations represent four ordinary differential equations for $[x_1^*(t), y_1^*(t)]$ and $[x_2^*(t), y_2^*(t)]$ and will not be given in detail here; one general first integral obtained[18] is

$$a^2 = y_1^* y_2^* \left[\frac{(x_1^* - x_2^*)^2 + (y_1^* - y_2^*)^2}{(x_1^* - x_2^*)^2 + (y_1^* + y_2^*)^2} \right] \tag{1}$$

Here a is a constant whose value is fixed once the initial location of the vortices is specified. The parameter a also has the following physical significance. For a given initial location (specified by given values of ℓ, b, and α in Fig. 1), the vortex trajectories are uniquely determined; depending on the sense of rotation of the vortices, the vortices will either approach or recede from the wall. At large distances from the wall, it is readily shown[18] that the vortex trajectories approach straight lines separated by a distance $2a$. The parameter a is thus characteristic of the trajectories and is a convenient length scale to use in defining the following dimensionless variables:

$$x = x^*/a, \qquad y = y^*/a, \qquad t = |\kappa| t^*/a^2 \tag{2}$$

where t^* measures dimensional time from the introduction of the vortices into the flow.

In addition to Eq. (1), a further result that follows from the trajectory equations[18] is that the vertical distance between vortices remains constant; this distance is thus fixed by the initial location of the vortex pair and, denoting the dimensionless separation distance by ϵ, it follows that

$$\epsilon = y_1 - y_2 \tag{3}$$

and Eq. (1) becomes

$$y_1 y_2 \left[\frac{(x_1 - x_2)^2 + (y_1 - y_2)^2}{(x_1 - x_2)^2 + (y_1 + y_2)^2} \right] = 1 \tag{4}$$

Both these relations must hold at each point on the trajectory. In particular, at the initial location (Fig. 1), it can be shown,

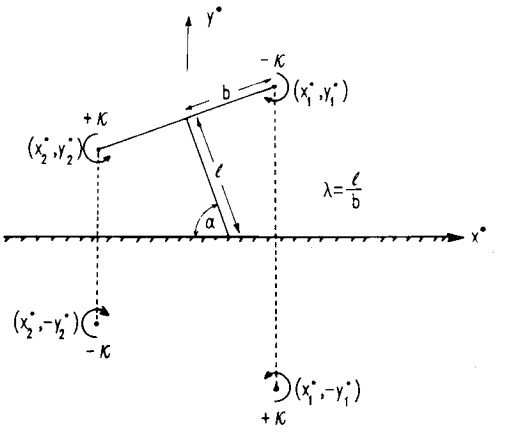

Fig. 1 Coordinate system and initial vortex configurations; image vortices are below the wall.

using Eq. (4), that (ℓ, b, α) are related to ϵ by

$$\epsilon = 2\cos\alpha\left(\frac{\lambda^2+1}{\lambda^2-\cot^2\alpha}\right)^{\frac{1}{2}} \tag{5}$$

where $\lambda = \ell/b$. Consequently, the trajectory depends on only two of the three parameters: ϵ (the dimensionless separation distance), α (the angle of attack), and λ (the initial ratio of total separation distance to distance from the wall). Once two parameters are specified, the third may be obtained from Eq. (5) and the trajectories are fixed.

At large distances from the wall, the trajectories approach straight lines inclined at an angle β to the wall; it may be verified using Eq. (3) that β is related to ϵ by

$$\beta = \arccos\left(\frac{\epsilon}{2}\right) \tag{6}$$

in the range $0 < \epsilon < 2$. In this range of ϵ, the trajectories are as indicated in Fig. 2. Note that values of $\epsilon > 2$ are also possible;[18] in such cases the vortex paths are rather different than those depicted in Fig. 2; the vortices move toward one another along paths almost parallel to the wall and then experience a perturbation in the path (sometimes in the form of a loop) as they pass.[18] In this paper, only the range $0 < \epsilon < 2$ is considered (for which $0 < \beta < 90$ deg); note, from Fig. 2, that the angle of approach of the trajectory β is generally less than the angle of attack α (corresponding to the starting location).

It can be shown[18] that the trajectory equations in dimensionless form can be written

$$\frac{dy_+}{dt} = -\frac{1}{2}\left[\frac{4+\epsilon^2-y_+^2}{\epsilon^2-y_+^2}\right]^2\left[\frac{\epsilon^2-y_+^2(\epsilon^2-4)}{y_+^2-4-\epsilon^2}\right]^{\frac{1}{2}} \tag{7}$$

$$\frac{dx_+}{dt} = \epsilon\left[\frac{1}{2}+\frac{4}{\epsilon^2-y_+^2}\right] \tag{8}$$

Here $y_+ = y_1 + y_2$ and $x_+ = x_1 + x_2$. Equations (7) and (8) may be integrated numerically, starting from the initial conditions

$$y_+(0) = \lambda\epsilon\tan\alpha, \qquad x_+(0) = -\lambda\epsilon \tag{9}$$

for specified values of λ, α [ϵ is obtained from Eq. (5)]. It follows from Eq. (4) that

$$x_2 - x_1 = \left[\frac{\epsilon^2-y_+^2(\epsilon^2-4)}{y_+^2-4-\epsilon^2}\right]^{\frac{1}{2}} \tag{10}$$

and, consequently, once a numerical solution of Eqs. (7) and (8) is carried out, values of (x_1, y_1) and (x_2, y_2) at all values of t may be obtained using Eqs. (3) and (10). The numerical integrations were carried out using a fourth-order Runge-Kutta method with very small time steps in order to ensure good accuracy.

As the vortices move along the trajectory, they induce an unsteady tangential velocity near the wall given by

$$U_\infty(x,t) = U_1(x,t) + U_2(x,t) \tag{11}$$

Here U_1 and U_2 are the velocities induced by vortices 1 and 2, respectively, and their images, namely,

$$U_1(x,t) = \frac{2y_1\,\mathrm{sgn}(\kappa)}{(x-x_1)^2+y_1^2}, \qquad U_2(x,t) = \frac{-2y_2\,\mathrm{sgn}(\kappa)}{(x-x_2)^2+y_2^2} \tag{12}$$

Here $\mathrm{sgn}(\kappa)$ denotes the sign associated with the circulation of vortex 1 (Fig. 1). At any stage, (x_1, y_1) and (x_2, y_2) are known (as numerical functions) from the solution of Eqs. (7) and (8); thus U_∞, in Eq. (11) is an explicit function of x and an implicit function of t. It is evident from Eqs. (12) that since vortex 2 is closest to the wall, it will generally make the largest contribution to the tangential velocity near $x = x_2$ for small y_2.

III. Boundary-Layer Formulation

With the tangential velocity near the wall given by Eq. (11), the inviscid solution is not uniformly valid, and an unsteady boundary layer exists on the wall in order to satisfy the no-slip condition; the boundary-layer problem is formulated in this section. A Reynolds number for this flow may be defined according to

$$Re = |\kappa|/\nu \tag{13}$$

where ν is the kinematic viscosity. Dimensionless boundary-layer variables may be defined by

$$x = x^*/a, \qquad y' = y^* Re^{\frac{1}{2}}/a, \qquad t = t^*|\kappa|/a^2$$
$$u = au^*/|\kappa|, \qquad v = av^* Re^{\frac{1}{2}}/|\kappa| \tag{14}$$

where (u^*, v^*) denote velocities tangential and normal to the wall, respectively. The unsteady laminar boundary-layer equations are then

$$\frac{\partial u}{\partial t} + u\frac{\partial u}{\partial x} + v\frac{\partial u}{\partial y'} = \frac{\partial U_\infty}{\partial t} + U_\infty\frac{\partial U_\infty}{\partial x} + \frac{\partial^2 u}{\partial y'^2}$$
$$\frac{\partial u}{\partial x} + \frac{\partial v}{\partial y'} = 0 \tag{15}$$

where U_∞ is given by Eqs. (11) and (12). The boundary conditions associated with Eqs. (15) are

$$u = v = 0 \text{ at } y' = 0, \qquad u \to U_\infty \text{ as } y' \to \infty \tag{16}$$

It is now convenient to introduce two transformations that are useful in the numerical solution of Eqs. (15).

Consider first the following transformation to a new streamwise coordinate ξ according to

$$\xi = \frac{2}{\pi}\arctan\left[\frac{2x - x_1(t) - x_2(t)}{x_1(t) - x_2(t)}\right] \tag{17}$$

where x_1 and x_2 are the instantaneous streamwise locations of the vortices. This transformation is one-to-one and maps the doubly infinite range of $x(-\infty, \infty)$ to a finite range in ξ of $(-1, 1)$; this is a desirable feature for the numerical solu-

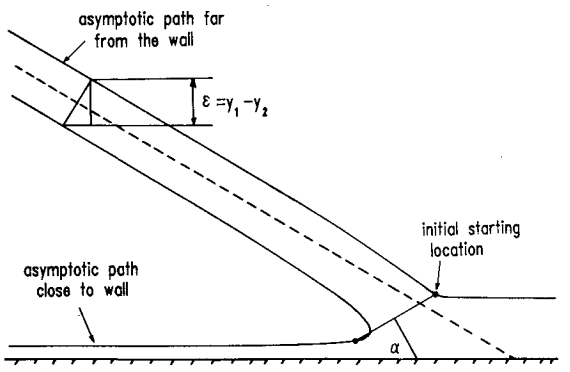

Fig. 2 Typical vortex trajectories for $0 < \epsilon < 2$ showing the relation of the initial location to the asymptotic paths.

tion approach. A second important characteristic of Eq. (17) is that it transforms the position of the first and second vortices to $\xi = \pm 1/2$, respectively, for all t; thus, although the vortices move in the x space, they are frozen in the ξ coordinate. In addition, the range in ξ of $(-1/2, +1/2)$, corresponding to the region between the vortices where the important boundary-layer effects are expected to occur, is emphasized by the transformation; on the other hand, the regions at large distances from the vortices are de-emphasized. For these reasons, a uniform mesh spacing on a finite range in the ξ coordinate may be adopted, and this is very convenient in the numerical solution.

A second transformation is necessitated by the behavior of the boundary-layer solution at the initiation of the motion. For a given value of ϵ (or equivalently β), the trajectory of the pair is fixed (see Fig. 2); however, the vortex pair may be started at any location on the trajectory, and the initial location is fixed by specifying a value of λ. Once the vortices are inserted on the trajectory at $t = 0$, a thin, unsteady boundary layer having a thickness $0(t^{\frac{1}{2}})$ starts to form on the wall. In order to take this irregular behavior into account, it is convenient to introduce a new variable η by

$$\eta = y'/(2t^{\frac{1}{2}}) \tag{18}$$

Furthermore, the tangential component of velocity is written according to

$$u = U_1(x,t)\operatorname{erf}\eta + U_2(x,t)\frac{\partial \Psi}{\partial \eta} \tag{19}$$

where $\Psi(\xi, \eta, t)$ is the dependent variable to be determined. The normal velocity component takes the form

$$v = -2\sqrt{t}\frac{\partial \xi}{\partial x} \times \left[\frac{\partial U_1}{\partial \xi}\left(\eta\operatorname{erf}\eta + \frac{e^{-\eta^2}}{\sqrt{\pi}} - \frac{1}{\sqrt{\pi}}\right) + \frac{\partial U_2}{\partial \xi}\Psi + U_2\frac{\partial \Psi}{\partial \xi}\right] \tag{20}$$

where ξ is given by Eq. (17) and U_1 and U_2 are given by Eqs. (12). The detailed motivation for the form of Eq. (19) is discussed in detail elsewhere.[18] Essentially the dominant contribution to the tangential velocity at the boundary-layer edge is provided by U_2, and the variable $\partial\Psi/\partial\eta$, defined by Eq. (19), is a normalized velocity that varies from zero to one across the boundary layer.

Defining a normalized tangential velocity U by

$$U = \frac{\partial \Psi}{\partial \eta} \tag{21}$$

the boundary-layer equations (15), with the transformation equations (17-19), may be written in the form

$$4t\frac{\partial U}{\partial t} = \frac{\partial^2 U}{\partial \eta^2} + P\frac{\partial U}{\partial \eta} + RU + Q\frac{\partial U}{\partial \xi} + G \tag{22}$$

where

$$P = 2\eta + 4t \times \left[\frac{\partial U_1}{\partial x}\left(\eta\operatorname{erf}\eta + \frac{e^{-\eta^2}}{\sqrt{\pi}} - \frac{1}{\sqrt{\pi}}\right) + \frac{\partial U_2}{\partial x}\Psi + U_2\frac{\partial \xi}{\partial x}\frac{\partial \Psi}{\partial \xi}\right] \tag{23}$$

$$R = -4t\left[\frac{1}{U_2}\frac{\partial U_2}{\partial t} + \frac{U_1}{U_2}\frac{\partial U_2}{\partial x}\operatorname{erf}\eta + \frac{\partial U_1}{\partial x}\operatorname{erf}\eta + \frac{\partial U_2}{\partial x}U\right] \tag{24}$$

$$Q = -4t\left[\frac{\partial \xi}{\partial t} + U_1\frac{\partial \xi}{\partial x}\operatorname{erf}\eta + U_2 U\frac{\partial \xi}{\partial x}\right] \tag{25}$$

$$G = \frac{4t}{U_2}\left[\frac{\partial U_\infty}{\partial t} + U_\infty\frac{\partial U_\infty}{\partial x} - \frac{\partial U_1}{\partial t}\operatorname{erf}\eta - U_1\frac{\partial U_1}{\partial x}\operatorname{erf}^2\eta + \frac{2}{\sqrt{\pi}}e^{-\eta^2}U_1\frac{\partial U_1}{\partial x}\left(\eta\operatorname{erf}\eta + \frac{e^{-\eta^2}}{\sqrt{\pi}} - \frac{1}{\sqrt{\pi}}\right) + \frac{2e^{-\eta^2}}{\sqrt{\pi}}U_1\frac{\partial U_2}{\partial x}\Psi + \frac{2e^{-\eta^2}}{\sqrt{\pi}}U_1U_2\frac{\partial \xi}{\partial x}\frac{\partial \Psi}{\partial \xi}\right] \tag{26}$$

Note that Eq. (22) is nonlinear since the coefficients in Eqs. (23-26) contain the dependent variables U and Ψ; Eq. (22) is simply a convenient form for a numerical solution of the boundary-layer problem. The gradients of U_1, U_2, and ξ with respect to x and t may be obtained by differentiation of Eqs. (12) and (17) and, using the differential equations of motion for (x_1, y_1), (x_2, y_2), analytic expressions for the required gradients are readily obtained. The boundary conditions associated with Eqs. (21) and (22) are

$$U(\xi,0) = \Psi(\xi,0) = 0; \qquad U(\xi,\eta) \to 1, \quad \text{as } \eta \to \infty \tag{27}$$

for all ξ.

At large distances from the vortices ($\xi \to \pm 1$), the boundary layer develops independently from the rest of the boundary-layer flow, and Eq. (22) becomes

$$4t\frac{\partial \tilde{U}}{\partial t} = \frac{\partial^2 \tilde{U}}{\partial \eta^2} + P\frac{\partial \tilde{U}}{\partial \eta} + \tilde{R}\tilde{U} + \tilde{G} \tag{28}$$

where the tilde has been used to denote U at upstream or downstream infinity ($\xi \to \pm 1$); the limiting values of the coefficients are

$$\tilde{P} = 2\eta, \qquad R = -4t\frac{\dot{y}_2}{y_2}, \qquad \tilde{G} = 4t\frac{\dot{y}_1}{y_2}\operatorname{erf}\eta \tag{29}$$

where the dot indicates differentiation with respect to t. The boundary conditions for $\tilde{U}$ are also given by Eqs. (27).

IV. The Numerical Solution

The vortices may be introduced into the flow at any instant and will then move continuously on trajectories similar to those depicted in Fig. 2. Once the vortices are introduced, a thin boundary layer starts to form on the wall; the limit of Eq. (22) as $t \to 0^+$ is

$$\frac{\partial^2 U}{\partial \eta^2} + 2\eta\frac{\partial U}{\partial \eta} = 0 \tag{30}$$

and the solution satisfying Eqs. (27) is

$$U = \operatorname{erf}\eta, \qquad \Psi = \eta\operatorname{erf}\eta + \frac{e^{-\eta^2}}{\sqrt{\pi}} - \frac{1}{\sqrt{\pi}} \tag{31}$$

This is the initial solution from which the boundary-layer flow develops forward in time. Note that if the vortices are inserted at large distances from the wall, the boundary-layer flow development is very gradual until the vortices approach the wall within a distance comparable to the initial separation distance of the vortices. For this reason, most of the cases considered in this study were started with the vortices relatively close to the wall.

The numerical procedure used to advance the solution of Eq. (22) forward in time is based on a Crank-Nicolson

method[14,15,18] as well as an alternative approach[15] designed for situations in which the boundary-layer flow begins to develop strong outflows. A rectangular grid was defined in the (ξ, η) plane with uniform mesh spacings denoted by (h_1, h_2), respectively. A number of mesh sizes were used as a check on the accuracy, and it was determined that values of $h_1 = 0.01$ and $h_2 = 0.05$ were sufficiently small. The last of Eqs. (27) must be enforced on a large but finite value of η and, typically, a value of $\eta_\infty = 6$ was determined to be adequately large. Thus, in a typical calculation, there were 201 mesh points in the ξ direction and 121 points in the η direction.

The numerical problem is to advance the solution forward in time from the initial condition given by Eq. (31). In the early stages of the motion, variations with respect to time are quite large; therefore rather small time steps were used initially. In a typical calculation, ten initial time steps with $\Delta t = 10^{-3}$ were used; then four steps with $\Delta t = 5 \times 10^{-3}$ were carried out, and finally a constant time step of $\Delta t = 10^{-2}$ was used thereafter. In order to advance the solution in time, it is necessary to compute the solution at the left and right boundaries ($\xi = \pm 1$), respectively and to this end, the solution of Eq. (28) was calculated using a standard Crank-Nicolson method. At each time step, once the solution of Eq. (28) had been advanced, the finite difference equations corresponding to the discretization of Eq. (22) were solved iteratively using relaxation methods.[15,18] Typically, 10–15 iterations were required to obtain convergence at a time step; this was deemed to have occurred when successive iterates at all interior mesh points agreed to within four significant figures.

In the latter stages of the integrations after boundary-layer separation occurred, variations in the flowfield became so intense that the matrix problem associated with the Crank-Nicolson method failed to remain diagonally dominant and the iterative scheme failed to converge. In such cases, the alternate differencing method discussed by Doligalski and Walker[15] was used. The technique is a variation of the conventional Crank-Nicolson method in which only the differencing of the terms $P\partial U/\partial\eta$ and $Q\partial U/\partial\xi$ in Eq. (22) is affected. In the normal manner,[15] Eq. (22) is approximated at the midpoint between the current time plane at t and the previous time plane at $t - \Delta t$. Let function values at $t - \Delta t$ and $t - \Delta t/2$ be denoted by single and double asterisks, respectively; in the alternate differencing scheme,[15] the approximation to $Q\partial U/\partial\xi$ depends on the local sign of Q_{ij}^{**}, where subscripts i, j denote a typical point in the (ξ, η) plane, and

$$Q\frac{\partial U}{\partial \xi} = \frac{Q_{ij}^{**}}{2h_1}\{U_{i+1,j} - U_{ij} + U_{ij}^{*} - U_{i-1,j}\} \qquad (32)$$

for $Q_{ij}^{**} > 0$ with

$$Q\frac{\partial U}{\partial \xi} = \frac{Q_{ij}^{**}}{2h_1}\{U_{ij} - U_{i-1,j} + U_{i+1,j}^{*} - U_{ij}^{*}\} \qquad (33)$$

for $Q_{ij}^{**} < 0$; similarly for the term $P\partial U/\partial\eta$,

$$P\frac{\partial U}{\partial \eta} = \frac{P_{ij}^{**}}{2h_2}\{U_{i,j+1} - U_{ij} + U_{ij}^{*} - U_{i,j-1}\} \qquad (34)$$

for $P_{ij}^{**} > 0$ and

$$P\frac{\partial U}{\partial \eta} = \frac{P_{ij}^{**}}{2h_2}\{U_{ij} - U_{i,j-1} + U_{i,j+1}^{*} - U_{ij}^{*}\} \qquad (35)$$

for $P_{ij}^{**} < 0$. The main feature of this technique is that differencing of the convective terms in the current time plane is carried out in a manner related to the local direction of the flow. This approach always yields a matrix that is diagonally dominant and in addition is second-order accurate in both space and time. This approach could be used to push the calculations further in time; however, with the onset of explosive growth within the boundary layer, it should be noted that the second scheme ultimately failed as well.

V. Calculated Results

A variety of cases were considered[18] corresponding to different rotations, initial locations, and angles of attack; here some results for four cases will be considered and further details and cases may be found in Ref. 18. The first case considered here corresponds to vortices having the rotation indicated in Fig. 1, which therefore move toward the wall. In order to define a trajectory and an initial location, it is necessary to define any two of the parameters α, β, and λ; since $\lambda = \ell/b$ (Fig. 1), increasing values of λ correspond to either 1) increasing the initial distance from the wall for fixed b or 2) decreasing the separation of the vortices for fixed ℓ.

To obtain a clear physical picture of the flowfield, the streamline patterns in the boundary layer are presented in terms of the physical coordinate x rather than the coordinate ξ used in the numerical integrations. In the subsequent plots, the instantaneous streamlines are plotted with the flow direc-

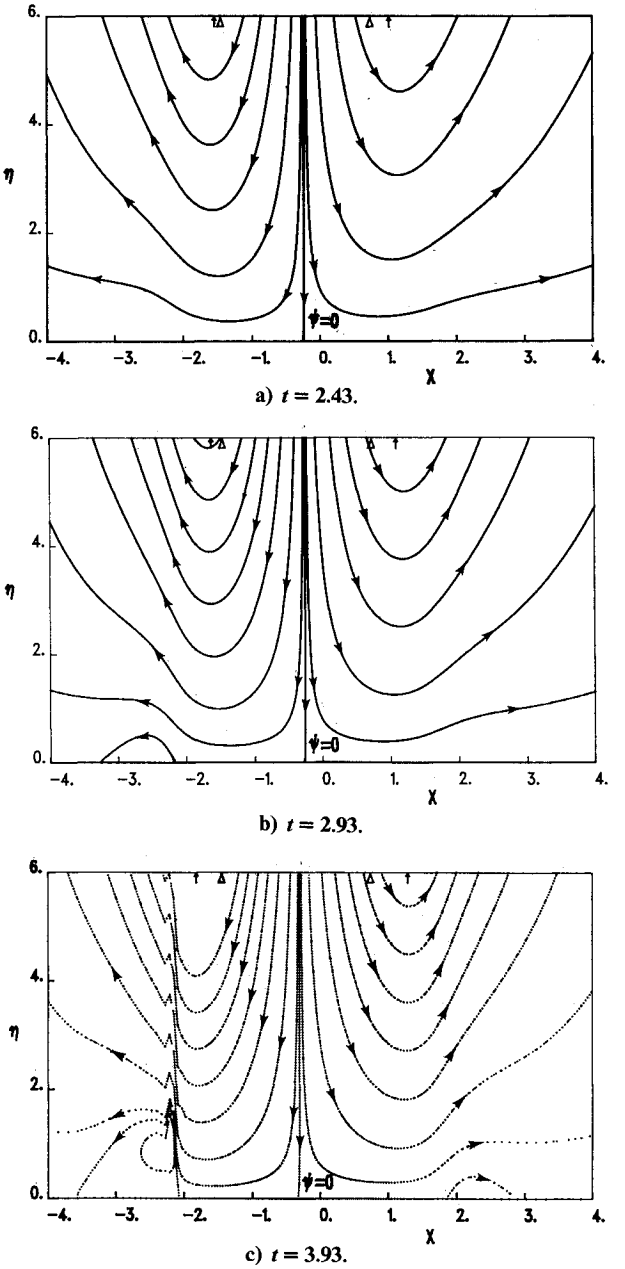

a) $t = 2.43$.

b) $t = 2.93$.

c) $t = 3.93$.

Fig. 3 Instantaneous boundary-layer streamlines for a downward-moving pair ($\alpha = 81$ deg, $\beta = 80$ deg, $\lambda = 2.107$).

tion indicated by arrows. As a useful point of reference, the initial streamwise locations of the two vortices are indicated by an open triangle at the top of the graph; the current vortex locations are indicated by a vertical arrow.

For the first case, $\alpha = 81$ deg, $\beta = 80$ deg, and the vortices are started relatively far from the wall with $\lambda = 2.107$. The instantaneous streamlines at $t = 2.43$ are shown in Fig. 3a. It may be observed that the downward-moving vortex pair induces a boundary-layer flow that is almost symmetrical. However, the lifting of the streamlines near $x = -3$ hints at the onset of boundary-layer separation that has developed by $t = 2.93$ in Fig. 3b. As t increases and the pair moves closer to the wall, the secondary eddy in the left portion of the boundary layer develops and grows; the stagnation point on the wall on the right side of the eddy exhibits little movement while the left stagnation point moves progressively in the direction of x decreasing. Near the right side of the eddy, the variations in the flowfield become progressively more intense as time increases and the boundary layer begins to thicken rapidly. At the next stage of development in Fig. 3c at $t = 3.93$, it may be observed that a spikelike behavior has developed in the streamlines. Note that a second separation has occurred in the right portion of the boundary layer.

In order to extend the calculations to the point depicted in Fig. 3c, it was necessary to abandon the Crank-Nicolson integration scheme and to adopt the alternate differencing scheme.[15,18] Note, however, that at this stage, the numerical mesh is not fine enough to cope adequately with the rapidly intensifying flow variations near the right side of the more mature secondary eddy. In this region, rapid boundary-layer growth occurs after separation, and this may be seen in the temporal development of the displacement velocity plotted in Fig. 4; this quantity is defined as

$$V_{\text{disp}} = \lim_{y' \to \infty} V_{\text{b.l.}} - \lim_{y \to 0} V_{\text{I}} \tag{36}$$

where $V_{\text{b.l.}}$ and V_{I} denote the vertical velocities in the boundary-layer and inviscid regions, respectively. Effectively, V_{disp} is the normal velocity induced at the boundary-layer edge by events that take place within the boundary layer. Using Eq. (20), it can be shown[17] that

$$Re^{\frac{1}{2}} V_{\text{disp}} = 2\sqrt{t}\left[\frac{1}{\sqrt{\pi}}\frac{\partial U_1}{\partial x} + \frac{\partial U_2}{\partial x}\lim_{\eta \to \infty}(\eta - \Psi) - U_2 \lim_{\eta \to \infty}\frac{\partial \Psi}{\partial x}\right] \tag{37}$$

It may be observed from Fig. 4 that the latter stages of the integration are characterized by increasingly strengthening boundary-layer outflows near the left secondary eddy. It is clear that this boundary-layer flow is evolving toward a state of interaction with the outer flow. At present, methods to compute this type of strong interaction are not known (other than full Navier-Stokes calculations) and, consequently, it has not been possible to compute the interaction. However, the experimental results of Harvey and Perry[12] suggest that a strong inviscid-viscous interaction will occur in the form of the ejection of the left secondary eddy from the boundary-layer region.

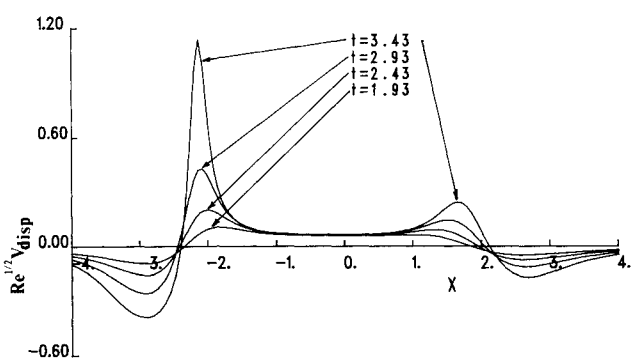

Fig. 4 Temporal development of displacement velocity for the boundary-layer flow of Fig. 3.

It may be observed from Fig. 4 that strengthening outflows are occurring near the right secondary eddy as well; however, the boundary layer is evolving toward interaction near the left secondary eddy before the process matures near the right eddy. This behavior was found to be typical of situations where a vortex pair moves toward a wall;[18] the vortex closest to the wall always induces a separation, and the flow moves rapidly toward an interactive state. At shallower angles of attack, this process usually occurs before the vortex furthest from the wall can induce a separation. Consequently, the vortex closest to the wall always dominates the evolution of the boundary-layer flow. In all cases, a boundary-layer eruption in the form of an ejected secondary eddy is expected; this eddy will have the opposite sense of rotation to vortex 2 (Fig. 1), and the eruption will occur to the left of the current streamwise location of vortex 2. These conclusions are in agreement with the observed behavior of the boundary layer induced by a vortex loop approaching a wall.[10,11,17]

If the rotations of all the vortices in Fig. 1 are reversed, $\text{sgn}(\kappa) = -1$ [see Eq. (12), for example], and the vortices recede from the wall along a trajectory similar to that depicted in Fig. 2; such situations are now considered. In the second case discussed in this paper, $\alpha = 68$ deg, $\beta = 60$ deg, and the vortex pair is started relatively close to the wall with $\lambda = 1.2852$. The instantaneous streamlines in the boundary layer are plotted in Fig. 5a at $t = 0.83$, where it may be observed that separation has occurred. A comparison with Fig. 3a should be made; note that the direction of the flow is reversed

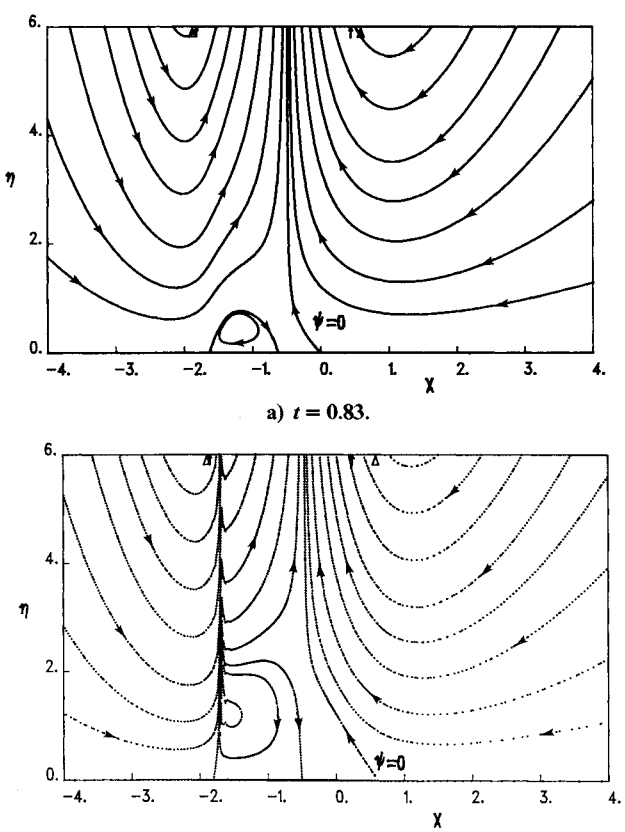

Fig. 5 Instantaneous boundary-layer streamlines for an upward-moving pair ($\alpha = 68$ deg, $\beta = 60$ deg, $\lambda = 1.285$).

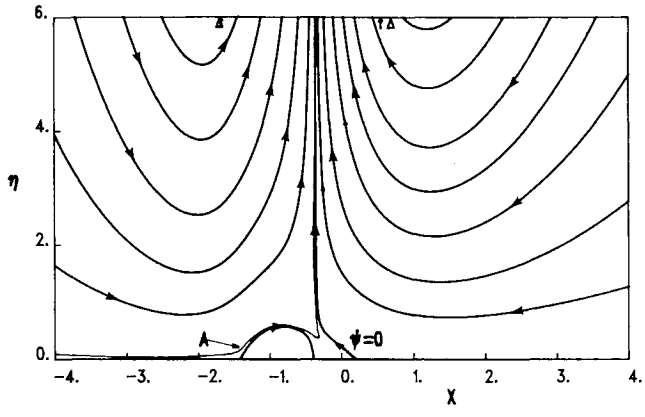

a) $t = 0.93$.

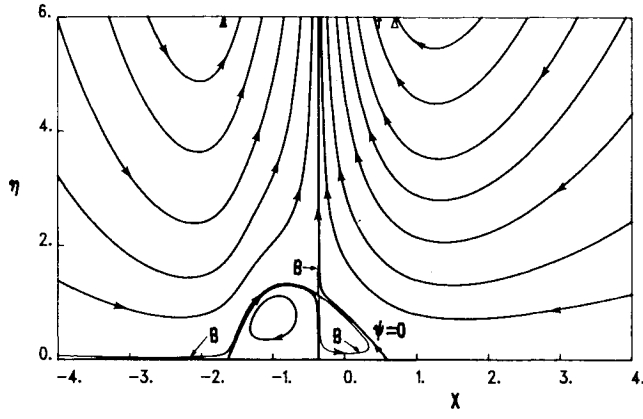

b) $t = 1.43$.

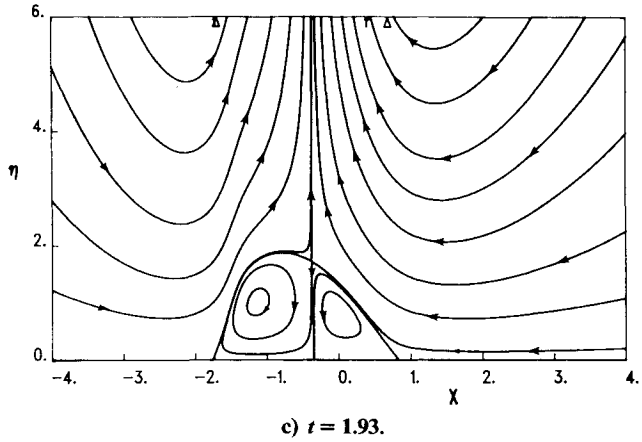

c) $t = 1.93$.

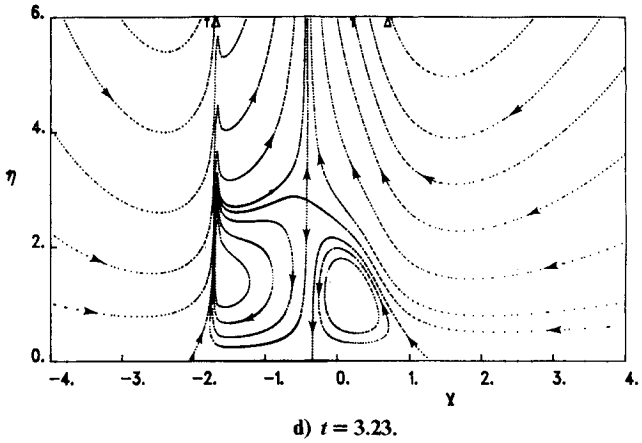

d) $t = 3.23$.

Fig. 6 Instantaneous boundary-layer streamlines for an upward-moving pair ($\alpha = 74$ deg, $\beta = 70$ deg, $\lambda = 1.448$).

as the upward-moving vortex pair brings the boundary-layer fluid toward the $\psi = 0$ streamline and upward. In addition, the secondary eddy now occurs in a region inboard of vortex 2. As time increases, the left stagnation point of the secondary eddy exhibits little movement, while the right stagnation point moves progressively to the right. As the eddy grows in a direction normal to the wall, the streamlines on the left side of the eddy are distended to an increasing extent as the boundary-layer fluid must climb over a rapidly growing region of recirculating flow. The streamlines at $t = 1.83$ are shown in Fig. 5b; at this point it may be observed that the variations in the boundary-layer flowfield are very intense. To extend the solution to the point in Fig. 5b, it was necessary to use the alternate differencing scheme; however, it is evident from Fig. 5b that the solution is suffering from numerical inaccuracies, and shortly after $t = 1.83$ the alternate differencing scheme failed to converge as well. The reason for the failure is believed to be associated with the onset of a singular behavior at finite time[19] as the boundary-layer flow moves toward an interaction with the order flow. At the stage indicated in Fig. 5b, the displacement velocity exhibits[18] explosive boundary-layer growth near the left side of the secondary eddy. In this case, the expected form of the viscous-inviscid interaction is an ejection of the single secondary eddy from a region inboard of vortex 2 and between the rising vortex pair.

In the next case considered, a somewhat different boundary-layer development is obtained when the angle of approach of the trajectory is increased to $\beta = 70$ deg; the values of the other parameters were taken to be $\alpha = 74$ deg and $\lambda = 1.448$. The instantaneous streamlines at $t = 0.93$ are plotted in Fig. 6a at $t = 0.93$, where it may be observed that separation has occurred. The streamline labeled A follows along the top of the secondary eddy and then enters the region between the right side of the eddy and the zero streamline; the A streamline then reverses course and follows the zero streamline toward the top of the boundary layer. The behavior of the A streamline is typical of those streamlines that enter the gap between the right side of the eddy and the zero streamline; at the next stage of development depicted in Fig. 6b at $t = 1.43$, it may be observed that another secondary eddy has formed in this region. The streamline defining this eddy is labeled B in Fig. 6b. Streamline B rides over the top of the first secondary eddy before reaching a stagnation point; the rest of the B streamline defines the boundary of the second eddy as well as a portion that rises toward the inviscid region. Note that for the two secondary eddies, the first (or left) eddy is attached to the wall, while the right eddy is detached at this stage.

With time, the streamline patterns in Fig. 6b undergo an interesting development. The streamline defining the edge of the right attached eddy and the $\psi = 0$ streamline pull successively together near the stagnation point on streamline B until all three streamlines are almost coincident at about $t = 1.63$. At this stage, a change occurs near the stagnation point and the zero streamline attaches to the wall; in addition, the right secondary eddy becomes detached from the wall. The complete sequence is documented in detail in a sequence of plots at short intervals near $t = 1.63$ in Ref. 18. The streamlines at $t = 1.93$ are plotted in Fig 6c. It may be seen that the left eddy, which was originally attached to the wall, has become detached; on the other hand, the originally detached right eddy becomes attached to the wall. As time increases, the boundary-layer flow evolves toward becoming interactive with the outer flow on the left side of the left secondary eddy. The liftup and distention above the left side of the secondary eddy in Fig. 6c is a precursor of the behavior depicted in Fig. 6d in the terminal stages of the integration for this case. Although two secondary eddies are present in this boundary-layer flow, the strongest outflows are associated with the left secondary eddy; this eddy developed first in the boundary layer under the vortex that is closer to the wall. The temporal development of displacement velocity is plotted in Fig. 7, where it

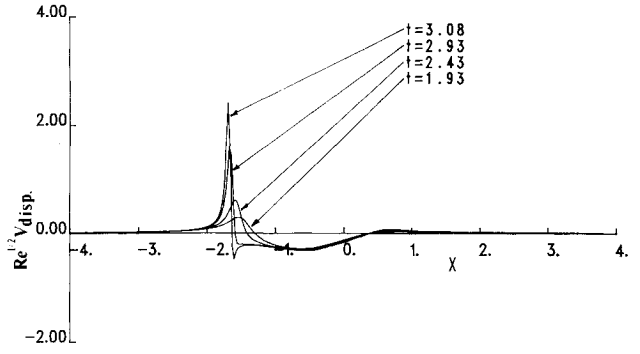

Fig. 7 Temporal development of the displacement velocity for the boundary-layer flow of Fig. 6.

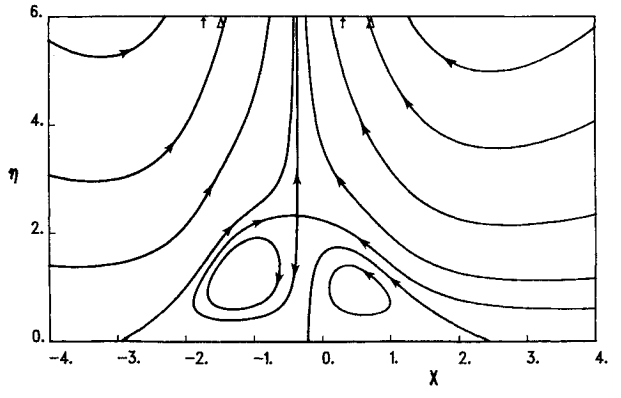

Fig. 8 Instantaneous boundary-layer streamlines for an upward-moving pair at $t = 4.93$ ($\alpha = 81$ deg, $\beta = 80$ deg, $\lambda = 2.107$).

may be confirmed that explosive growth is occurring on the left side of the detached secondary eddy; an eruption of the boundary-layer flow is expected in this region.

In the final case considered here, the angle of approach was increased to $\beta = 80$ deg, and the vortices were started relatively far from the wall with $\alpha = 81$ deg and $\lambda = 2.1071$. In this case the moving pair induces a separation in the boundary layer, and this is illustrated in Fig. 8 at $t = 4.93$. The numerical integrations in such cases may evidently be continued on indefinitely. Although outflows are induced in the boundary layer, they are relatively weak, and there is no evidence of the onset of explosive boundary-layer growth. As the vortices recede farther from the wall, their influence on the boundary layer wanes and, in this case, the vortices are apparently able to escape from the wall region without inducing a boundary-layer eruption.

VI. Summary and Conclusions

The present results indicate that whenever a vortex pair is in motion near a wall, boundary-layer separation will occur near the wall; furthermore, the boundary-layer flow is usually dominated by the influence of the vortex closest to the wall. When the vortices move toward the wall, a single secondary eddy occurs first in a streamwise location outboard of the vortex closest to the wall. The streamlines on the right side of the secondary eddy soon develop a pronounced distention (Fig. 3b) as they are forced to climb over a growing region of recirculating flow. This behavior is a clear indication of the onset of explosive boundary-layer growth. As the boundary layer moves toward an interaction with the outer flow, a singularity is expected to evolve in the boundary-layer solution at finite time;[15,16,19] it is believed that this is the reason why the numerical integrations ultimately failed. Essentially, the singular behavior develops as a consequence of the attempt in the present calculation method to impose the pressure gradient due to the vortices on the boundary layer for an indefinite period of time. It is clear that it will be necessary to develop an interactive strategy to be able to compute the flowfield, once explosive boundary-layer growth starts to develop. At present this has not been possible; however, experiments indicate[12,13] that the interaction is in the form of ejection of the secondary eddies from the boundary layer.

For vortex pairs that recede from the wall, separation first occurs to the right of the vortex closest to the wall. For cases at shallow angle of approach ($\beta \leq 60$ deg), the effects of the vortex closest to the wall completely dominate the development of the boundary-layer flow; separation occurs in the form of a single eddy attached to the wall and the flow moves rapidly toward interaction on the left side of this secondary eddy. As the angle of approach is increased, a rather novel separation phenomenon occurs. First, a single secondary eddy appears, which is attached to the wall; then, another secondary eddy occurs to the right, which is detached from the wall. As the parent vortices move farther away from the wall, the two secondary eddies react in a complicated way with the result that the left eddy detaches from the wall while the right eddy attaches. The boundary-layer flow then moves toward interaction, in this case, on the left side of the more mature eddy. Finally, it has also been demonstrated that if the vortices are initially far from the wall, separation is still induced in the boundary layer but an interaction apparently will not occur.

The majority of the flows discussed in this paper appear ultimately to lead to a strong unsteady viscous-inviscid interaction, which is expected to take the form of an eruption and ejection of secondary vortices. It is clearly desirable to develop computational methods that can handle such strong interactions, and this is an important area for future research.

Acknowledgment

The authors are grateful for support of this work under AFOSR Contract F49620-83-K-0033.

References

[1]Head, M.R. and Bandyophadyay, P., "New Aspects of Turbulent Boundary Layer Structure," *Journal of Fluid Mechanics*, Vol. 107, June 1981, pp. 297-337.

[2]Smith, C.R., "A Synthesized Model of the Near-Wall Behavior in Turbulent Boundary Layers," *Proceedings of the Eighth Symposium on Turbulence*, edited by G.K. Patterson and J.L. Zakin, University of Missouri Rolla, 1984.

[3]Acarlar, M.S. and Smith, C.R., "An Experimental Study of Hairpin-Type Vortices as a Potential Flow Structure of Turbulent Boundary Layers," Dept. of Mechanical Engineering, Lehigh University, Bethlehem, PA, Rept. FM-5, Oct. 1984.

[4]Blackwelder, R.F., "The Bursting Process in Turbulent Boundary Layers," *Coherent Structure of Turbulent Boundary Layers*, edited by C.R. Smith and D.E. Abbott, Lehigh University, Bethlehem, PA, 1978, pp. 211-227.

[5]Blackwelder, R.F., "Analogies Between Transitional and Turbulent Boundary Layers," *Physics of Fluids*, Vol. 26, Oct. 1983, pp. 2807-2815.

[6]Beljars, A.C.M., Krishna Prasad, K., and DeVries, A.A., "A Structural Model for Turbulent Exchange in Boundary Layers," *Journal of Fluid Mechanics*, Vol. 112, Nov. 1981, pp. 33-70.

[7]Ersoy, S. and Walker, J.D.A., "Viscous Flow Induced by Counter-rotating Vortices," *Physics of Fluids*, Vol. 28, Sept. 1985, pp. 2687-2698.

[8]Doligalski, T.L. and Walker, J.D.A., "Shear Layer Breakdown Due to Vortex Motion," *Coherent Structure of Turbulent Boundary Layers*, edited by C.R. Smith and D.E. Abbott, Lehigh University, Bethlehem, PA, 1978, pp. 288-339.

[9]Falco, R.E., "Coherent Motions in the Outer Region of Turbulent Boundary Layers," *Physics of Fluids*, Vol. 20, Oct. 1981, pp. S124-S132.

[10]Falco, R.E. and Wiggert, R.E., "Effects of Dilute Polymer Solutions on Vortex Ring/Wall Interactions—A Mechanism for Drag Reduction," *Progress in Astronautics and Aeronautics*: edited by G. Hough, Vol. 79, AIAA, New York, 1980, pp. 275-289.

[11]Falco, R.E., "A Synthesis and Model of Turbulence Structure in the Wall Region," *Structure of Turbulence in Heat and Mass Transfer*,

edited by Z.P. Zaric, Hemisphere Publishing Corp., New York, 1982, pp. 43-57.

[12]Harvey, J.K. and Perry, F.J., "Flowfield Produced by Trailing Vortices in the Vicinity of the Ground," *AIAA Journal*, Vol. 9, Aug. 1971, pp. 1659-1660.

[13]Mehta, R.D. and Lim, T.T., "Flow Visualization Study of a Vortex/Wing Interaction," NASA TM 86656, Oct. 1984.

[14]Walker, J.D.A., "The Boundary Layer Due to a Rectilinear Vortex," *Proceedings of the Royal Society of London Series A*, Vol. 359, Feb. 1978, pp. 167-188.

[15]Doligalski, T.L. and Walker, J.D.A., "The Boundary Layer Induced by a Convected Two-Dimensional Vortex," *Journal of Fluid Mechanics*, Vol. 139, Feb. 1984, pp. 1-28.

[16]Sears, W.R. and Telionis, D.P., "Boundary Layer Separation in Unsteady Flow," *SIAM Journal of Applied Mathematics*, Vol. 28, Feb. 1975, pp. 215-235.

[17]Cerra, A.W. and Smith, C.R., "Experimental Observation of Vortex Ring Interactions with Fluid Adjacent to a Surface," Dept. of Mechanical Engineering, Lehigh University, Bethlehem, PA, Rept. FM-4, 1983.

[18]Ersoy, S., "The Viscous Flow Induced Near a Wall by Counter-Rotating Vortex Pairs and Vortex Loops," Ph.D. Dissertation, Lehigh University, Bethlehem, PA, June 1985.

[19]VanDommelen, L.L. and Shen, S.F., "The Spontaneous Generation of a Singularity in a Separating Laminar Boundary Layer," *Journal of Computational Physics*, Vol. 38, Nov. 1980, pp. 125-140.